Int. J. Econ. Environ. Geol., Vol. 17, Issue 3, 2026, 151-160 doi: 10.46660/int.j.econ.environ.geol..v17i3.871.
Journal home page: www.econ-environ-geol.org

ADSORPTIVE REMOVAL OF METHYLENE BLUE FROM AQUEOUS SOLUTION USING DALBERGIA SISSOO LEAF POWDER AS A LOW-COST BIOSORBENT

MAH E SAYYAM[1], SALEEM NAWAZ[1], SABEELA AMEEN[2], MUHAMMAD HAROON KHAN[1], HAFIZA SABA[3], ANIS SAFIR[4]*, BAI-BUREH O'BAI KAMARA[5, 6] AND ALI RAZA[7]

[1]Department of Chemistry, Islamia College University, Peshawar, Pakistan
[2]Department of Agriculture Sciences, University of Maples Federico II via Universit`a 100, 80055, Portici, Napoli, Italy
[3]Department of Environmental Sciences, Government College University, Lahore, Pakistan
[4]College of New Energy and Environment, Jilin University, Changchun, 130021, China
[5]Magbosi Land Water and Environment Research Center (MLWERC) Mile91, Sierra Leone, West Africa
[6]Agriculture Department, Central University, Sierra Leone, West Africa
[7]Institute of Soil and Environmental Sciences, University of Agriculture, Faisalabad, Pakistan

Received: *4 August, 2026* ***Accepted:*** *10 September, 2026*

Abstract: In this study, *Dalbergia sissoo* leaf powder (DSLP) was evaluated as a plant-waste adsorbent for methylene blue (MB) removal from water. SEM, EDS, and FTIR characterization revealed a rough, irregular surface and functional groups (–OH, –NH, C=O, and C=C). Small FTIR shifts (approximately 4 cm^{-1}) provided tentative evidence of their involvement in dye binding. Batch experiments examined initial dye concentrations (27–68 mg/L), adsorbent doses, and contact times (15–60 min). Adsorption capacity increased with dye concentration, ranging from 2.82 to 7.50 mg/g. The highest removal in the contact-time experiment (73.98%) occurred at 45 min; however, equilibrium time could not be precisely established. In the dose experiment, removal peaked at 61.74% with 0.3 g adsorbent before decreasing at 0.4 g, potentially due to particle aggregation. Adsorption capacity decreased with increasing dose. Langmuir, Freundlich, Temkin, and Dubinin–Radushkevich (D–R) models were evaluated. Langmuir fitted poorly and yielded non-physical parameters, preventing reliable determination of maximum monolayer capacity. Freundlich (R^2 = 0.978) and Temkin (R^2 = 0.968) showed comparatively better fits than D–R (R^2 = 0.913). However, only four concentrations were tested, limiting model discrimination. The low D–R mean adsorption energy (E = 0.516 kJ/mol) tentatively suggests physical interactions. The pseudo-second-order model (R^2 = 0.93) fitted better than the pseudo-first-order model (R^2 = 0.84), although this does not establish the adsorption mechanism. Overall, DSLP demonstrates potential as a low-cost adsorbent for dye-contaminated wastewater.

Keywords: Plant-based adsorbent, characterization heterogeneous surface, functional groups, dyes.

Introduction

The discharge of industrial wastewaters containing synthetic dyes is a major environmental challenge because of their recalcitrance, toxicity, and resistance to conventional treatments. Textile, printing, and other related industries' effluents substantially impact water quality by blocking sunlight and interfering with aquatic photosynthetic processes, thereby affecting the ecosystem (Khan *et al*., 2022; Wang *et al*., 2022).

Methylene blue (MB) is a cationic thiazine dye that finds extensive applications as a textile dye, paper dye and pharmaceutical agent. But its release into the aquatic environment could be a potential ecological and health concern as it is toxic and stable (Jawad *et al*., 2020).

Adsorption is a simple, efficient and economical process that has proven to be one of the most effective technologies for treatment of dyes (Crini *et al*., 2021). Isotherms (e.g. Langmuir, Freundlich, D-R and Temkin) are frequently used to describe equilibrium, representing multilayer adsorption on energetically non-uniform surfaces such as natural and biomass-based materials (Ayawei *et al*., 2021).

Recently, biomass-derived adsorbents have received significant attention as natural and environmentally friendly due to their availability, renewability and sustainability.

Recent research highlights the fact that plant-based adsorbents can be a viable waste-to-resource opportunity in line with sustainable water treatment technologies (Bassyouni *et al*., 2022). Yet, while a lot of research has been done on agricultural waste, very little has been done on leaf-based adsorbents in terms of their interactions and surface heterogeneity (Ahmad *et al*., 2021). Dalbergia sissoo is a common tree found in South Asia, and therefore offers a potential source of lignocellulosic biomass. The leaves

*Corresponding author e-mail: anissafir2019@gmail.com
© SEGMITE

contain abundant phenolic and oxygen-rich functional groups, and are likely to have a high affinity for cationic dyes like MB. However, there is a lack of studies on the adsorptive and surface reactivity of modified Dalbergia sissoo leaf powder, particularly from a surface geochemical point of view. Specifically, interactions between the distribution of functional groups, surface heterogeneity and adsorption mechanisms are poorly understood (Khatun *et al*., 2024).

Present study focuses on adsorptive removal of MB dye from water using modified DS leaf powder, and examines its equilibrium and kinetic behaviour. Nawaz *et al*. (2024) studied acid-activated Dalbergia sissoo leaf powder and its magnetic composite for the removal of the anionic dye alizarin red S. The present work applies modified DS leaf powder to the cationic dye MB over 27–68 mg/L. The contribution is therefore, limited to a different dye–adsorbent combination, and the adsorption capacity obtained is modest.

Materials and Methods

Adsorbent Preparation

The DSLP was prepared using the co-precipitation procedure based on the method reported by Nawaz *et al*. (2024), with the preparation details described below. Briefly, $FeSO_4 \cdot 7H_2O$ and $FeCl_3 \cdot 6H_2O$ were dissolved in distilled water under continuous stirring at 70–80°C. A 25% ammonia solution was added gradually to adjust the suspension to pH 10, after which 1 g of the prepared leaf-derived material was introduced. The suspension was stirred and allowed to cool, and the resulting solid was washed and dried at 60°C before grinding.

Stock Solution Preparation

A 100 mg/l methylene blue stock solution was prepared by dissolving 0.025g of methylene blue in 250 ml of deionized water. Working solutions were prepared using standard dilution ($C_sV_s = C_dV_d$) (Pathania *et al*., 2017).

Characterization of Adsorbent

Adsorbent's functional groups, surface morphology and elemental distribution before and after adsorption were analyzed using FTIR, SEM coupled with EDS respectively. U-V visible spectrophotometer was used for the determination of the adsorption efficiency.

Batch Adsorption Analysis of Methylene Blue

In a batch adsorption experiments, 50 mL of solution was shaken in the 100 mL conical flask at 200 r.p.m. The effects of initial MB concentration, adsorbent dose, and contact time were investigated in separate experimental series. Following each experiment, the adsorbent was separated from the solution by filtration, and the residual MB concentration was determined spectrophotometrically at 664 nm. Independent experimental replicates were not performed, and dye-only and adsorbent-only blank tests were not conducted.

Equations (1) and (2) were used to calculate the percent removal (%) and maximum uptake capacity (qe in mg/g) of MB.

Equation (1): Adsorption capacity

$$q_e = \frac{(C_0 - C_a)V}{m}$$

Equation (2): Percentage removal

$$\%Removal = \frac{(C_0 - C_a)}{C_0} X\ 100$$

Adsorption Isotherms

Adsorption equilibrium data were fitted to the linear forms of the Langmuir (Eq. 3 and 4) (Langmuir, 1932):, Freundlich (Eq. 6) (Freundlich, 1909), Dubinin–Radushkevich (D-R) (Eq. 7–9) (Chabani *et al*., 2006), and Temkin (Eq. 10) (Itodo, 2010) isotherm models.

$$X = \frac{bKCw}{1 + KCw} \quad \text{Eq. (3)}$$

$$\frac{Cw}{X/m} = \frac{1}{Kb} + \frac{Cw}{b} \quad \text{Eq. (4)}$$

$$x/m = K_f C_w^{\frac{1}{\beta}} \quad \text{Eq. (5)}$$

$$\log x/m = \log K_f + \frac{1}{\beta} \log C_w \quad \text{Eq. (6)}$$

$$\ln(q_e) = \ln(q_m) - \beta\varepsilon^2 \quad \text{Eq. (7)}$$

$$\varepsilon = \mathrm{RT} \ln\left[1 + \frac{1}{C_e}\right] \quad \text{Eq. (8)}$$

$$\mathcal{E} = \frac{1}{\sqrt{2\beta}} \quad \text{Eq. (9)}$$

$$q_e = \frac{RT}{BT} lnKT + \frac{\mathrm{RT}}{BT} lnC_e \quad \text{Eq. (10)}$$

Adsorption Kinetics of Metals

The kinetic experiment's results were fitted in pseudo-first (PFO) and second order (PSO) kinetic equations as shown in eq 11 and 12 (Mouni *et al*., 2018; Al-Asadi *et al*., 2023).

$$q_t = q_e(1 - e^{-k_1 t}) \quad \text{Eq. (11)}$$

$$q_t = \frac{qe^2.k_2.t}{1 + q_e.k_2.t} \quad \text{Eq. (12)}$$

Results and Discussion

Characterization of Adsorbent

The SEM micrographs illustrating the surface structure of DSLP before and after MB adsorption are presented in Figures 3.1(a) and 3.1(b), respectively. It was observed from SEM image before adsorption that the surface of Dalbergia sissoo leaf powder was not uniform, rough and porous

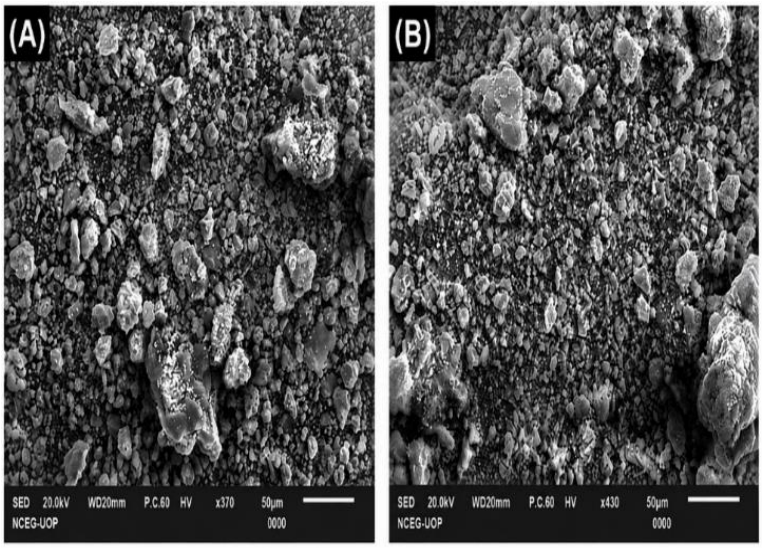
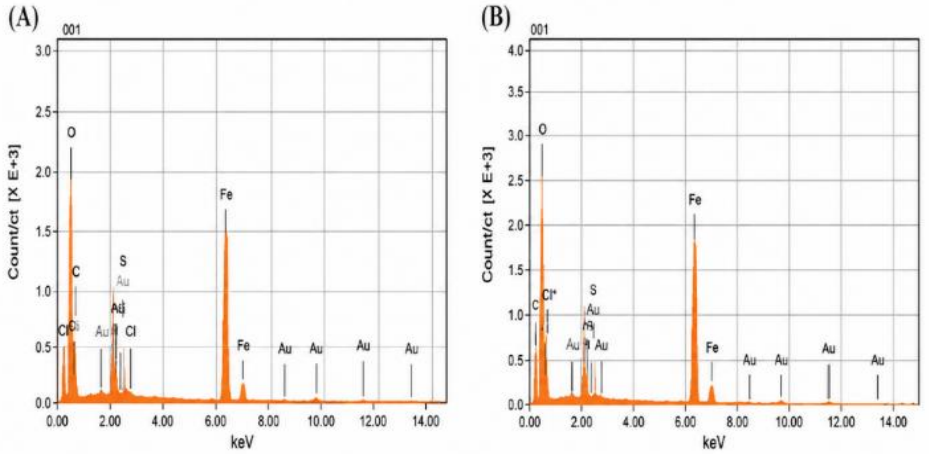


Fig. 1. SEM analysis of DS(A) before and (B) after adsorption.



Formula	mass%	Atom%	Sigma	Net	K ratio	Line
C	18.17	33.66	0.09	17543	0.0048471	K
O	34.43	49.16	0.10	57004	0.0719755	K
S*	0.28	0.27	0.02	2762	0.0012421	K
Cl	2.62	1.78	0.03	21149	0.0101238	K
Fe	38.03	15.24	0.13	108972	0.13418896	K
Au*	6.16	0.30	0.12	20277	0.0148100	M
Total	100.00	100.00				

Formula	mass%	Atom%	Sigma	Net	K ratio	Line
C	13.74	27.59	0.08	15558	0.0041871	K
O	34.58	52.10	0.09	70173	0.0595056	K
S*	0.10	0.07	0.02	707	0.0032305	K
Cl*	0.35	0.24	0.02	2632	0.0011238	K
Fe	44.39	19.16	0.14	130866	0.1652088	K
Au*	6.15	0.86	0.13	22588	0.0159672	M
Total	100.00	100.00				

Fig. 2. EDS spectra of DS (A) before and (B) after adsorption.

containing irregular shapes of particles, which could support the large number of active sites for adsorption of the dye. After adsorption, the surface morphology appeared smoother in some parts, which may be associated with the deposition of MB molecules on the adsorbent surface (Berta, 2024). However, SEM observations alone cannot confirm dye uptake or establish the presence of pores and adsorption sites quantitatively, particularly in the absence of BET surface-area measurements.

The EDS spectroscopy was performed on the elemental composition of the DSLP before and after adsorption is presented in the Figures (3.2(a,b)). After adsorption, similar elemental peaks were observed, however, noticeable variations in elemental composition occurred. The percentage of carbon content increased from 34.43% to 44.36% and the percentage of oxygen content increased from 18.17% to 30.50% after adsorption. Because MB ($C_{16}H_{18}N_3S^+Cl^-$) contains carbon, nitrogen, sulfur, and chlorine but no oxygen, the increase in oxygen content cannot be attributed directly to MB uptake. The increase in carbon content may be consistent with dye deposition, but this

interpretation requires caution because EDS percentages are relative measurements, and may change through normalization. Nitrogen, sulfur and chlorine would provide additional evidence of MB presence if their signals were reliably detected and quantified. Similar changes in elemental composition have been reported in previous adsorption studies (Farias Silva *et al*., 2020).

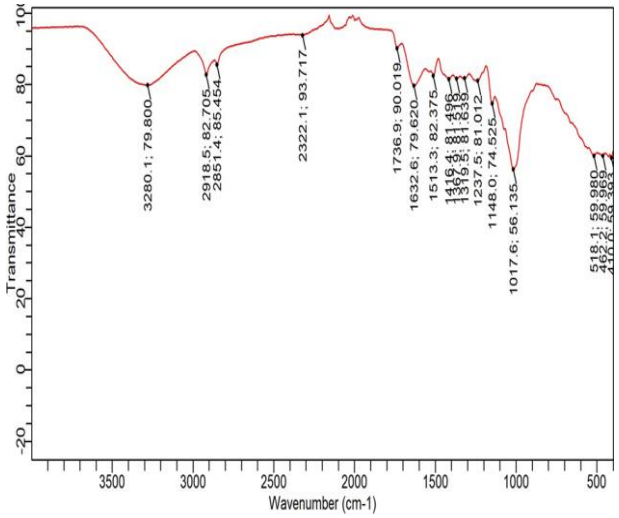


Fig. 3 (a) FTIR before adsorption of methylene blue.

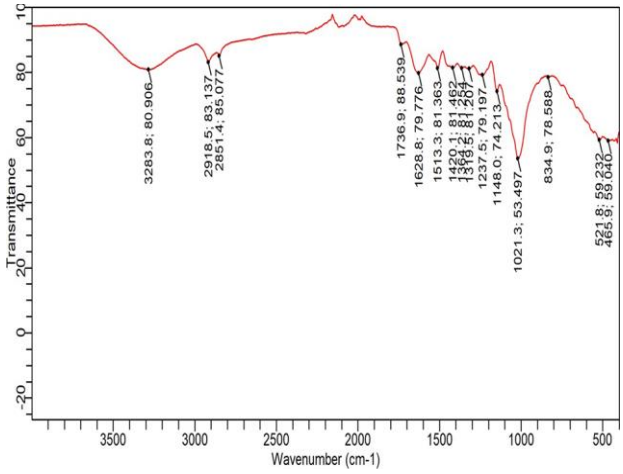


Fig. 3(b) FTIR after adsorption of methylene blue.

FTIR spectra of DSLP before and after adsorption of Methylene Blue, are presented in Figures 3.3(a,b), respectively. FTIR analysis, it was confirmed that there are several functional groups responsible for the adsorption. An adsorption band at 3280.1 cm^{-1} was observed over broad range before adsorption, and after adsorption the band was shifted to 3283.8 cm^{-1}, which corresponds to the stretching vibrations of hydroxyl (–OH) groups and may also indicate the presence of secondary amine (R_2NH) groups (Garg *et al*., 2025). The C=C stretching vibration before adsorption at 1632.6 cm^{-1} is red-shifted after the adsorption to 1628.8 cm^{-1}, and may also be due to carbonyl (C=O) functional groups (Pasieczna-Patkowska *et al*., 2025).

Following adsorption of Methylene Blue dye, there were significant changes in the position of some of the characteristic peaks which show interaction with the dye molecules, and with the active functional groups on the surface of the adsorbent material. The changes in the wave number before and after adsorption of MB dye are summarized in Table 3.1.

The participation of surface functional groups during adsorption is confirmed by peak shifts. The same FTIR peak changes after adsorption of dyes have been observed for biomass based adsorbents (Sadegh *et al*., 2019). Single beam UV-V spectrophotometry was used to determine the maximum absorption wavelength (λmax) of the Methylene Blue dye between the wavelength 400 – 750 nm. Hence, further adsorption assays and concentration measurements were taken in relation to the standard λmax of 664 nm for Methylene Blue dye (Hulupi *et al*., 2023).

Batch Equilibrium Studies

The calibration curve was constructed from four MB standards (27–68 mg/L) measured at 664 nm (Table 1, Fig. 4). The regression equation was A = 0.0065C + 0.285 (R^2 = 0.960), where A is absorbance and C is concentration (mg/L). This equation was used to calculate the residual dye concentration (C_e) in the adsorption experiments (Table 2) (Hamad & Idrus, 2022). Because the calibration is based on only four points, the calculated C_e and q_e values, particularly at low residual concentrations, should be regarded as approximate.

Table 1. Methylene blue absorbance at different concentrations.

Concentration (ppm)	Absorbance
27	0.47
40	0.52
54	0.66
68	0.72

Table 2. Initial concentrations, measured absorbance and calculated residual concentrations in the adsorption experiments

C_0 (mg/L)	Absorbance after adsorption	C_e (mg/L	Removal (%)
27	0.29	0.8	97.0
40	0.36	11.5	71.3
54	0.45	25.4	53.0
68	0.56	42.3	37.8

Effect of Initial Concentration

The initial concentration of MB was tested to be 27–68 mg/L with dose of 200 mg of adsorption agent and volume of 50 mL solution. The adsorption capacity (q_e) increased with the increase in the dye concentration, from 2.82 mg/g for 27 mg/L to 4.21 mg/g for 40 mg/L, 6.27 mg/g for 54 mg/L and maximum 7.50 mg/g for 68 mg/L (Fig. 5).

The equilibrium concentrations (C_e) were found to be 15.70, 23.14, 28.93 and 38.02 mg/L, respectively. This observed trend can be explained by the dye molecules becoming more available and the concentration gradient increasing, thus transfer of MB from the water to the adsorbent surface.

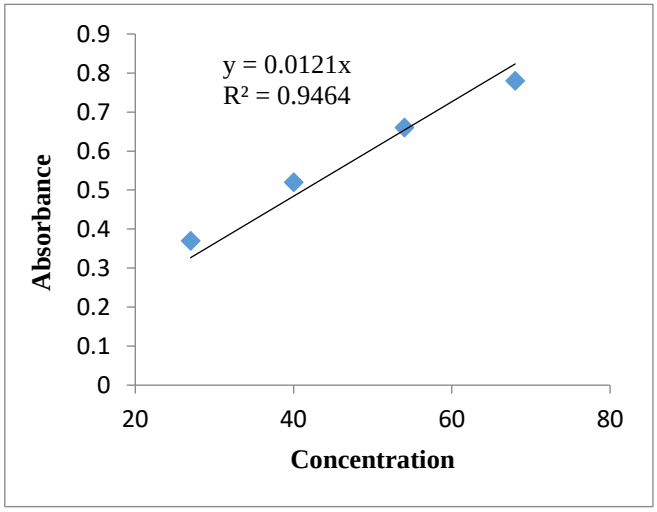


Fig. 4 Calibration plot of methylene blue illustrating the linear relationship between absorbance and concentration used for quantitative analysis.

The percentage removal was 41.84%, 42.15%, 46.43% and 44.09% at 27, 40, 54 and 68 mg/L, respectively, so it increased up to 54 mg/L and then decreased slightly. Therefore, 54 mg/L was selected for subsequent experiments. Ahmad *et al*. (2022) have reported similar trends in the past. Thus, further experiments were performed at 54 mg/L as the working concentration of the mixture (Khan *et al*., 2021).

Effect of Adsorbent Dose

The removal efficiency of MB under different adsorbent dosage (0.1–0.25 g) was investigated with a fixed MB concentration of 54 ppm (Fig. 6). The adsorption capacity (qe) is decreasing with the increase in the adsorbent dosage. However, the removal rate is initially enhanced with the increase of the dose of the adsorbent, reaching a peak at an intermediate dose, and then the removal rate decreases slightly at higher adsorbent dose.

Similarly, Hameed *et al*. (2009) reported that increasing the adsorbent dose improved MB removal efficiency but decreased the adsorption capacity (\(q_e\)). This decrease was attributed to the overlap of adsorption sites and aggregation of adsorbent particles, which reduced the effective availability of adsorption sites.

Effect of Contact Time

To understand the effect of contact time (15-60 min) on MB adsorption, it was carried out at the fixed concentration and adsorbent dosage (Fig. 7). The adsorption process is found to have good adsorption capacity (qe and % removal) with increase in time up to 45 minutes. The highest uptake was seen at 45 min within the range of 15-60 min. The reduction at 60 min could be because of partial desorption of weaker bound dye molecules but this is only tentative as the reduction may be within experimental error.

However, the early uptake period (time < 15 min) was not sampled and hence cannot be used to precisely define the equilibrium time from these four points. Kasbaji *et al*. (2023) documented a similar adsorption trend, with the adsorption of methylene blue using plant-based adsorbents usually taking between 30 and 60 min, and depending on the surface properties of the adsorbent material.

In earlier studies, it was also suggested that there is partial desorption of weakly bound dye molecules when shaking is prolonged (Gupta *et al*., 2021). A contact time of 45 min was thus chosen for subsequent experiments.

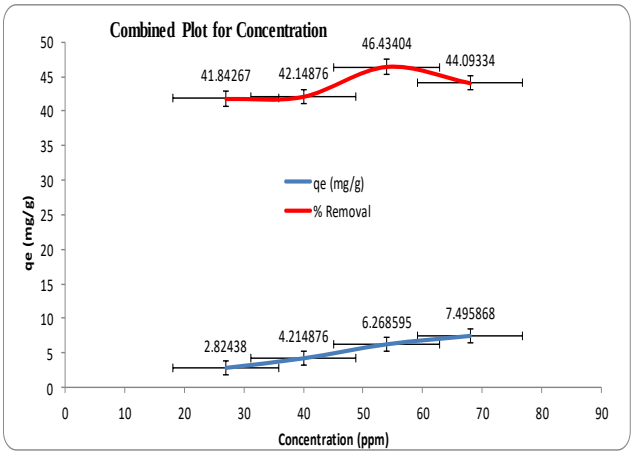


Fig. 5 Combined plot of adsorption capacity (**qe**) and percentage removal of Methylene Blue on DSLP at different initial MB concentration.

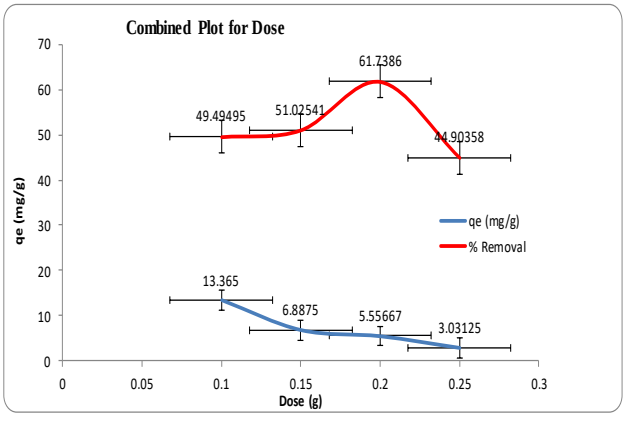


Fig. 6 Combined plot of adsorption capacity (qe) and percentage removal of Methylene Blue at different adsorbent doses using *DSLP*.

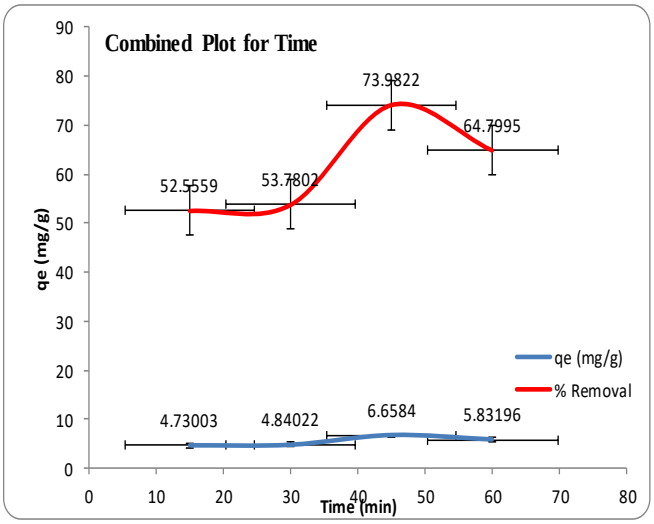


Fig. 7 Combined plot of adsorption capacity (qe) and percentage removal of methylene blue at different shaking times using *DSLP*.

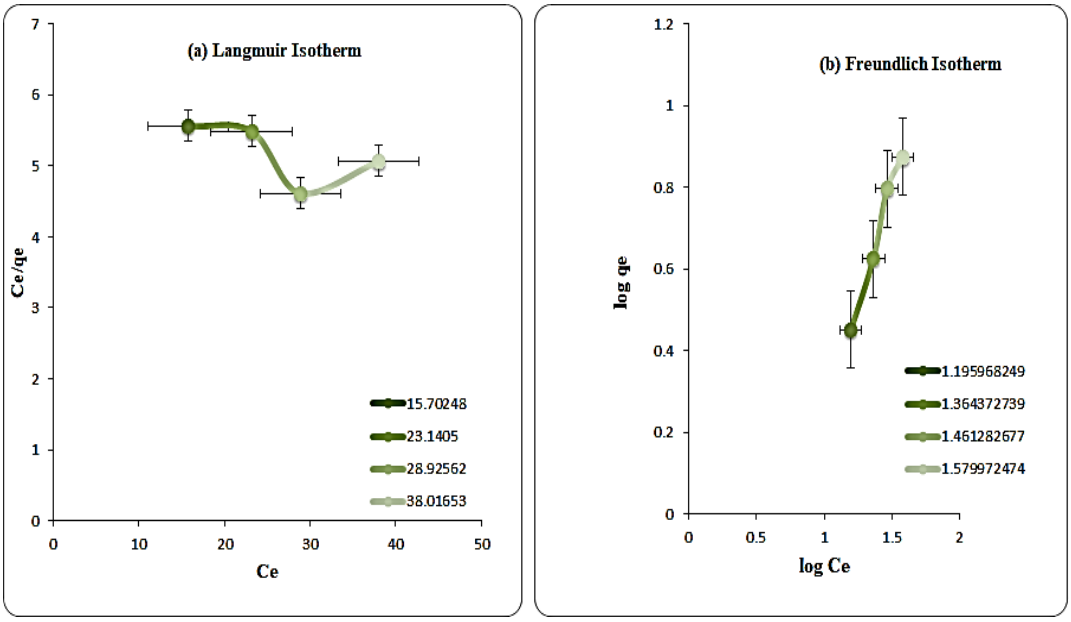


Fig. 8 Langmuir (a) and Freundlich (b) models applied to batch sorption experiment data of MB on DS.

Adsorption Models

The adsorption behaviour of methylene blue (MB) on DSLP was analysed with the Langmuir, Freundlich, Temkin and Dubinin–Radushkevich (D–R) isotherm models, to understand the adsorption mechanism, the surface characteristics and the possible interactions between the adsorbent and the adsorbate. Data were recorded using 4 isotherms when the data were linearized and the data obtained are displayed in Table 2 with the linear plots shown in Figures 8 and 9.

The Langmuir model did not give a good fit to the data (R^2 = 0.395). The linearized plot of C_e/q_e versus C_e (Fig. 8a) had a negative slope, giving q_m = −34.3 mg/g and K_L = −0.0049 L/mg (Table 2). The values are non-physical and R_L cannot be calculated and cannot be compared to the values of other adsorbents. A plateau was not reached within the range of concentrations tested, 27–68 mg/L, even at the highest concentration tested q_e values continued to increase (Fig. 5). These data do not allow for the determination of the maximum monolayer capacity, and the highest experimental

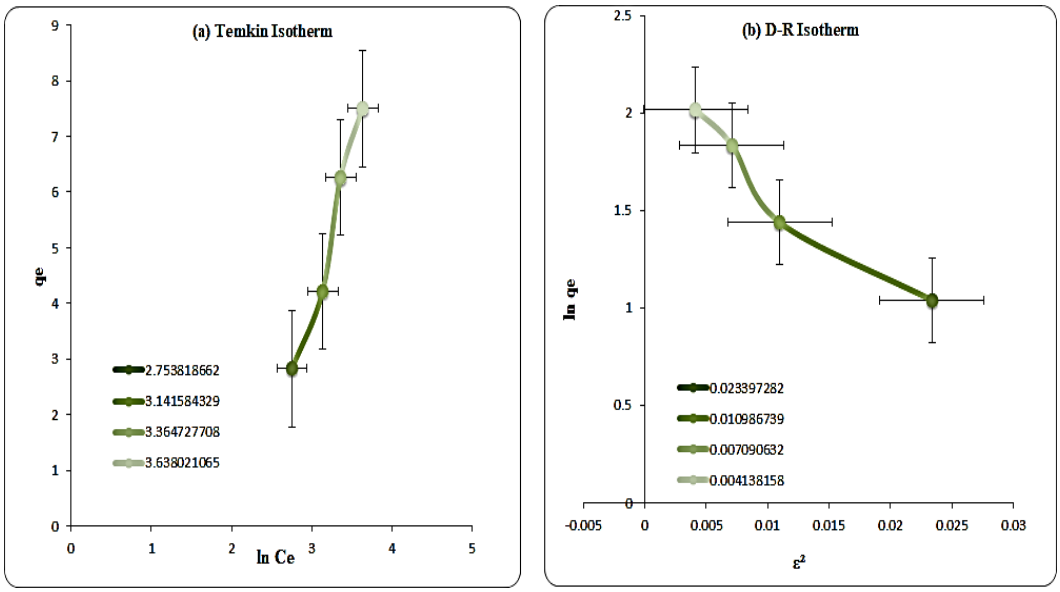


Fig. 9 Temkin (a) and D-R (b) models applied to batch sorption experiment data of MB on DS.

capacity (7.50 mg/g at 68 mg/L) can only be considered as a lower limit (Sulyman *et al*., 2017).

The Freundlich model gave a high coefficient of determination (R^2 = 0.978), with K_F = 0.119 (mg/g)(L/mg)^(1/n) and 1/n = 1.150 (Table 2). A value of 1/n greater than 1 for adsorption indicates unfavourable or cooperative adsorption in which the adsorption increases more than linearly with the concentration as opposed to the favourable adsorption. Multilayer adsorption is not necessarily indicated by a good Freundlich fit. This just confirms that the data are described by an empirical power law that is often encountered in heterogeneous surfaces (Sah *et al*., 2022). The same Freundlich isotherm has been observed for methylene blue adsorption with other biomass-based and agricultural-residue based adsorbents (Hamad & Idrus, 2022).

The Temkin model was another good fit (R^2 = 0.968). The slope of the plot of q_e vs ln C_e is the constant B, which is equal to 5.486 mg/g; the equilibrium binding constant K_T is 0.103 L/mg (Table 2). The results show strong interaction between MB and the adsorbent surface which is proved to be moderate (Verma *et al*., 2022).

The Dubinin–Radushkevich model gave R^2 = 0.913, with q_m = 8.41 mg/g and β = 1.88 mol² kJ^{-2} (Table 2). The mean adsorption energy, $E = 1/\sqrt{(2\beta)}$, was 0.516 kJ/mol. E<8 KJ/mol is less than the energy required for chemical adsorption, thus showing that the adsorption occurs physically (Hamad & Idrus, 2022). Due to the limited data the D–R parameters are indicative. In conclusion, the Freundlich model (R^2 = 0.978) and Temkin model (R^2 = 0.968) yielded similar high R^2 values with physical parameters while the Langmuir model yielded a low R^2 (0.395) with non-physical parameters, and the D–R model yielded R^2 = 0.913 with non-physical parameters. Four initial concentrations (N = 4) were employed and this restricts the ability to distinguish these between the models. Therefore the fit statistics should be taken with a pinch of salt and the adsorption mechanism cannot be determined from the fitting of the isotherms alone.

Table 4. Kinetic parameters for adsorption of methylene blue onto *Dalbergia sissoo* leaf powder.

Model	R^2	(qe) experimental (mg/g)	(qe) calculated (mg/g)	K (min^{-1})
Pseudo-first-order	0.84	7.48	6.21	0.041 (0.003)
Pseudo-second-order	0.93	7.48	7.51	0.018 (0.002)

Adsorption Kinetic Models

The adsorption mechanism and rate limiting steps of acid treated Dalbergia sissoo leaf powder were investigated by applying pseudo-first-order and pseudo-second-order models to analyze the adsorption kinetics of methylene blue. The kinetic plots are shown in Figures 10 and 11, and the parameters are given in Table 4. Pseudo-first-order model was not well suited to describe experimental data, as

indicated by its relatively low R^2 value (0.84), implying that this model did not accurately represent the adsorption process.

This model resulted in an equilibrium adsorption capacity of 6.21mg/g which is very different from the experimental adsorption capacity (q_e,exp) of 7.48mg/g. A pseudo first order rate constant (k_1) was calculated to be 0.041 min-1. The difference between the equilibrium adsorption capacity calculated, and experimental and lower R^2 value indicates that PFO did not adequately describe the adsorption of methylene blue on DS adsorbent (Pathania *et al*., 2017).

In contrast, pseudo-second order kinetic model could be more correlated with the experimental results, with an increase in the R^2 value to 0.93. The calculated adsorption capacity (q_e, cal = 7.51 mg/g) was found to be very close to experimental adsorption capacity (7.48 mg/g) and hence the model was found to be fitted very efficiently.

The pseudo-second order rate constant (k_2) was determined to be 0.018g mg−1 min−1. The pseudo-second order kinetic model gave the highest R^2 values and the best approximation of q_e compared to the experimental values, thus it was more suitable to describe the adsorption process. This may be because the methylene blue molecules are attracted to the surface of the adsorbent due to their functional groups.

The highest uptake occurred at 45 min within the 15-60 min range studied. Because no data were collected before 15 min, the initial uptake rate and the exact equilibrium time could not be resolved, and the apparent plateau may reflect the limited sampling rather than saturation of the sites. The adsorption of methylene blue from aqueous solution with different biomass and lignocellulosic adsorbents has also been reported to show a similar kinetic behavior (Tran *et al*., 2017).

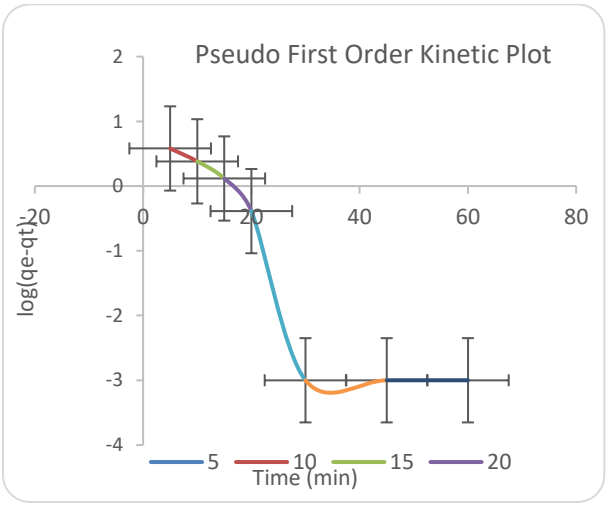


Fig. 10 Pseudo-first-order kinetic plot for adsorption of methylene blue onto *Dalbergia sissoo* leaf powder.

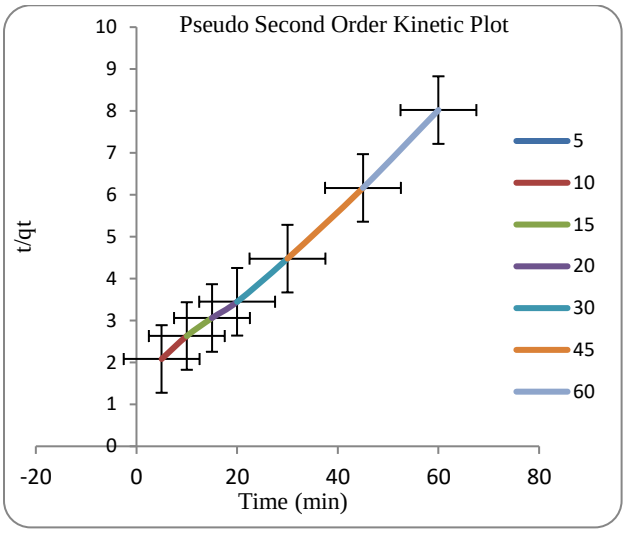


Fig. 11 Pseudo-second-order kinetic plot for adsorption of methylene blue onto *Dalbergia sissoo* leaf powder.

Conclusion

The outcomes of this study indicated that powdered DS leaf is suitable for use as an adsorbent to remove methylene blue from water and had a reasonable capacity (maximum experimental capacity 7.50 mg/g at 68 mg/L). The Freundlich (R2 = 0.978) and Temkin (R2 = 0.968) models both described the data similarly and by modelling, the data showed to have a moderate degree of equilibrium. The data exhibited a moderate degree of equilibrium as modelled by both the Freundlich (R2 = 0.978) and Temkin (R2 = 0.968) models. The goodness of Freundlich fit alone does not prove the multilayer adsorption (N = 4) and the models cannot be well discriminated with four concentrations. The Langmuir capacity could not be determined. The pseudo-second-order model (R2 = 0.93) was the best fitting model to the kinetic data as compared to the pseudo-first-order model (R2 = 0.84), but neither of these fits alone would confirm the mechanism. The mean free energy calculated using the D–R model (E = 0.516 kJ/mol) suggests that physical interactions may contribute to the adsorption process. However, this interpretation is tentative due to limited experimental data. Although DSLP is a readily available plant-waste material, its economic feasibility and reusability remain uncertain because no cost analysis or regeneration experiments were conducted.

Conflict of Interest

All the authors declared that there are no conflicts of interest.

Author's contribution

MS contributed in experimental work, data collection and manuscript preparation. SN supervised the study and provided the methodological guidance. MHK contributed in validation of results and manuscript review. AS and HS contributed in the manuscript writing and editing. SA

contributed in the interpretation of findings. BBOBK and AR critically reviewed the manuscript for submission. All authors read and approved the final manuscript for submission.

Acknowledgement

The authors would like to acknowledge their respective institutes for providing facilities and support to conduct this research.

References

Ahmad, M.J., Hameed, B.H. and Aziz, E.A. (2022). Surface modification of bentonite with surfactants for enhanced adsorption of pharmaceutical contaminants. *J. Environ. Chem. Eng.*, **10**(3): 107-118.

Ahmad, T., Rafatullah, M., Ghazali, A., Sulaiman, O., Hashim, R. and Ahmad, A. (2021). Removal of dyes using plant-based adsorbents: A review. *J. Environ. Manage.*, **284**: 112085.

Al-Asadi, S.T., Al-Qaim, F.F., Al-Saedi, H.F.S., Deyab, I.F., Kamyab, H. and Chelliapan, S. (2023). Adsorption of methylene blue dye from aqueous solution using low-cost adsorbent: kinetic, isotherm adsorption, and thermodynamic studies. *Environ. Monit. Assess.*, **195**(6): 676.

Ayawei, N., Ebelegi, A.N. and Wankasi, D. (2021). Modelling and interpretation of adsorption isotherms. *J. Chem.*, **2021**: 1-13.

Bassyouni, M., Abdel-Aziz, M.H., Zoromba, M.S., Abdel-Hamid, S.M. and Drioli, E. (2022). Sustainable adsorption technologies for wastewater treatment. *Sci. Total Environ.*, **805**: 150365.

Berta, H.M. (2024). Removal of methylene blue dye from aqueous solution using magnetite impregnated Khat Stem Nanocellulose Composites. *M.Sc. Thesis, Addis Ababa University, Ethiopia*, pp. 1-85.

Chabani, M., Amrane, A. and Bensmaili, A. (2006). Kinetic modelling of the adsorption of nitrates by ion exchange resin. *Chem. Eng. J.*, **125**(2): 111-117.

Crini, G., Lichtfouse, E., Wilson, L.D. and Morin-Crini, N. (2021). Conventional and non-conventional adsorbents for wastewater treatment. *Environ. Chem. Lett.*, **19**: 3761-3780.

Farias Silva, C.E., da Gama, B.M.V., da Silva Gonçalves, A.H., Medeiros, J.A. and de Souza Abud, A.K. (2020). Basic-dye adsorption in albedo residue: Effect of pH, contact time, temperature, dye concentration, biomass dosage, rotation and ionic strength. *J. King Saud Univ. Eng. Sci.*, **32**(6): 351-359.

Freundlich, H. (1909). Kapillarchemie. Eine Darstellung der Chemie der Kolloide und verwandter Gebiete. *Akademische Verlagsgesellschaft, Leipzig, Germany*, p. 948.

Garg, R., Dang, S. and Gauba, P. (2025). Molecular fingerprinting of heavy metal-resistant bacteria through FTIR analysis under heavy metal stress. *J. Pure Appl. Microbiol.*, **19**(1): 120-132.

Gupta, V.K., Nayak, A. and Agarwal, S. (2021). Adsorption of dyes using low-cost adsorbents: A review. *Water Resour. Ind.*, **25**: 100134.

Hamad, H.N. and Idrus, S. (2022). Recent developments in the application of bio-waste-derived adsorbents for the removal of methylene blue from wastewater: A review. *Polymers*, **14**(4): 783.

Hameed, B.H. and Ahmad, A.A. (2009). Batch adsorption of methylene blue from aqueous solution by agricultural waste. *J. Hazard. Mater.*, **164**(2-3): 468-472.

Hulupi, M., Keryanti, K., Rahmawati, K.A., Dewi, W.T. and Abdilah, F. (2023). Validation of methylene blue analysis method in wastewater samples by UV-Vis spectrophotometry. *Equilib. J. Chem. Eng.*, **7**(2): 101-106.

Itodo, A.U. and Itodo, H.U. (2010). Sorption energies estimation using Dubinin Radushkevich and Temkin adsorption isotherms. *Life Sci. J.*, **7**(3): 31-39.

Jawad, A.H., Abdulhameed, A.S. and Mastuli, M.S. (2020). Acid-factionalized biomass material for methylene blue adsorption. *J. Environ. Chem. Eng.*, **8**(5): 104379.

Khan, S., Naushad, M., Govarthanan, M., Iqbal, J. and Alfadul, S.M. (2022). Emerging contaminants of high concern for the environment: Current trends and future research. *Chemosphere*, **285**: 131335.

Khan, S., Rehman, F. and Ali, Z. (2021). Adsorption of methylene blue using agricultural waste biomass: Isotherm and kinetic studies. *Environ. Technol. Innov.*, **23**: 101718.

Khatun, H., Alam, S., Aziz, M.A., Karim, M.R., Rahman, M.H., Rabbi, M.A. and Habib, M.R. (2024). Plant-assisted green preparation of silver nanoparticles using leaf extract of *Dalbergia sissoo* and their antioxidant, antibacterial and catalytic applications. *Bioprocess Biosyst. Eng.*, **47**(8): 1347-1362.

Langmuir, I. (1932). Vapor pressures, evaporation, condensation and adsorption. *J. Am. Chem. Soc.*, **54**(7): 2798-2832.

Mouni, L., Belkhiri, L., Bollinger, J.C., Bouzaza, A., Assadi, A., Tirri, A. and Remini, H. (2018). Removal of Methylene Blue from aqueous solutions by adsorption on Kaolin: Kinetic and equilibrium studies. *Appl. Clay Sci.*, **153**: 38-45.

Nawaz, S., Salman, S.M., Ali, A., Ali, B., Shah, S.N. and Rahman, L.U. (2024). Kinetics and thermodynamics investigations of efficient and eco-friendly removal of Alizarin red S from water via acid-activated *Dalbergia sissoo* leaf powder and its magnetic iron oxide nanocomposite. *Front. Chem.*, **12**: 1457265.

Pasieczna-Patkowska, S., Cichy, M. and Flieger, J. (2025). Application of Fourier transform infrared (FTIR)

spectroscopy in characterization of green synthesized nanoparticles. *Molecules*, **30**(3): 684.

Pathania, D., Sharma, S. and Singh, P. (2017). Removal of methylene blue by adsorption onto activated carbon developed from *Ficus carica* bast. *Arab. J. Chem.*, **10**: S1445-S1451.

Sadegh, H., Ali, G.A.M., Agarwal, S. and Gupta, V.K. (2019). Surface modification of MWCNTs with carboxylic-to-amine and their superb adsorption performance. *Int. J. Environ. Res.*, **13**(3): 523-531.

Sah, M.K., Edbey, K., EL-Hashani, A., Almshety, S., Mauro, L., Alomar, T.S., AlMasoud, N. and Bhattarai, A. (2022). Exploring the biosorption of methylene blue dye onto agricultural products: A critical review. *Separations*, **9**(9): 256.

Kasbaji, M., Mennani, M., Boussetta, A., Grimi, N., Barba, F. J., Mbarki, M. and Moubarik, A. (2023). Bio-adsorption performances of methylene blue (MB) dye on terrestrial and marine natural fibers: Effect of physicochemical properties, kinetic models and thermodynamic parameters. *Sep. Sci. Technol.*, **58**(2): 221-240.

Sulyman, M., Namiesnik, J. and Gierak, A. (2017). Low-cost adsorbents derived from agricultural by-products/wastes for enhancing contaminant uptakes from wastewater: A review. *Pol. J. Environ. Stud.*, **26**(2): 479-510.

Tran, H.N., You, S.J., Hosseini-Bandegharaei, A. and Chao, H.P. (2017). Mistakes and inconsistencies regarding adsorption of contaminants from aqueous solutions: A critical review. *Water Res.*, **120**: 88-116.

Verma, R., Chahal, M. and Kumari, S. (2022). Exploration of biomass waste as low cost adsorbents for removal of methylene blue dye: A review. *Int. J. Environ. Anal. Chem.*, **102**(18): 6210-6235.

Wang, X., Jiang, J. and Gao, W. (2022). Reviewing textile wastewater produced by industries: characteristics, environmental impacts, and treatment strategies. *Water Science and Technology*, **85**(7): 2076-2096.

This work is licensed under a Creative Commons Attribution-Non Commercial 4.0 International License.